International Journal of Physical Sciences Vol. 4 (4), pp. 221-232, April, 2009
Available online at http://www.academicjournals.org/IJPS
ISSN 1992 - 1950 © 2009 Academic Journals

Full Length Research Paper

Speed-sensorless, adjustable-speed induction motor drive based on dc link measurement

S. B. Bodkhe[1]* and M. V. Aware[2]

[1]Department of Electrical Engineering, G. H. Raisoni College of Engineering, Digdoh-hill, Hingna-road Nagpur, Maharashtra, India 440 016.
[2]Department of Electrical Engineering, Visvesvarya National Institute of Technology, Bajaj-nagar, Nagpur, Maharashtra state, India 440 022.

Accepted 19 March, 2009

This paper presents a new control strategy for three-phase induction motor which includes speed and torque control loops and the current regulation thereby overcoming the limitation of volts per hertz control drives. For close-loop control, the feedback signals including the rotor speed, flux and torque are not measured directly but are estimated by means of an algorithm. The inputs to this algorithm are the reconstructed waveforms of stator currents and voltages obtained from the dc link and not measured directly on stator side. The proposed drive thus requires only one sensor in the dc link to implement the close-loop speed and torque control of a three-phase induction motor. Unlike the conventional flux and speed observers, the proposed estimation algorithm needs less computation and is less dependent on machine parameters. The proposed scheme is simulated using Matlab/Simulink software and is tested on a 2.2 kW drive for various steady-state and dynamic operating conditions. The results show fast dynamic response and good agreement between the actual values and the estimated values of torque and speed. Replacement of the open-loop control strategy of existing v/f drive by the proposed close-loop strategy appears to be possible without requiring any additional power components and sensors.

Key words: Speed-sensorless, estimation, dc link, reconstruction, three-phase induction motor, space-vector, band-pass filter.

INTRODUCTION

The widespread industrial use of induction motor (IM) has been stimulated over the years by their relative cheapness, low maintenance and high reliability. The control of induction motor variable speed drives (Bose, 2003) often requires control of machine currents, which is normally achieved by using a voltage source inverter Boussak and Jarray, 2006; Tzou and Hsu, 1997). A large number of control strategies have been (registered/developed so far (Comanescu and Xu, 2006; Hernafors et al., 2003; Rodic and Jezernik, 2002). The volts per hertz (v/f) induction motor drives with inverters are widely used in a number of industrial applications promising not only energy saving, but also improvement in productivity and quality.

The low cost applications usually adopt v/f scalar control when no particular performance is required. Variable-speed pumps, fans and appliances are the examples. Furthermore, these applications usually do not require zero-speed operation. The main advantage of v/f control is its simplicity and for this reason it has been traditionally implemented using low cost microcontrollers (Bajoi et al., 2008). For those applications which require higher dynamic performance than v/f control, the dc motor like control of IM that is called, the field oriented control (FOC) is preferred. The basic idea of FOC was first proposed in 1970s by using the rotor field oriented d-q coordinate system. The key issue for a FOC drive is how to obtain

*Corresponding author. E-mail: s_b_bodkhe@yahoo.co.in. Tel.: +919822718740. Fax: +91-07104-232560.

Symbols: suffix '*e*'- synchronous reference frame; suffix '*s*'- stationary reference frame; P, number of poles; R_s, stator resistance per phase (ohms); R'_r, rotor resistance per phase (ohms); L_m, magnetizing inductance (H); L_s, stator inductance (H); L'_r, rotor inductance (H).

the decoupled control of machine flux and torque. The indirect field oriented controlled IM drive is widely used in high performance applications due to its simplicity and fast dynamic response (Boldea and Nasar, 2006; Bose, 2003).

During the last few years, a particular interest has been noted on applying speed sensorless FOC to high performance applications that is based on estimation of rotor speed by using the machine parameters, instantaneous stator currents and voltages (Kwon and Kim, 2007; Maiti et al., 2008; Messaoudi et al., 2007; Nagata et al., 2008). The benefits of speed sensorless control are the increased reliability of overall system with the removal of mechanical sensors, thereby reducing sensor noise and drift effects as well as cost and size.

However, to exploit the benefits of sensorless control, the speed estimation methods must achieve robustness against model and parameter uncertainties over a wide speed range. Parameters of particular concern in the sensorless control literature are frequency-dependent R_r', temperature-dependent R_s and the load torque, all of which are very effective on the accurate estimation of flux and speed.

To address the parameter sensitivity problem in IM speed sensorless control, a variety of approaches have been proposed, that is, studies based on sliding mode observers by Derdiyok (2005), estimating the R_r' and Lascu et al. (2004), estimating the R_s; studies on speed adaptive flux observers as done by Guidi and Umida (2000), in which R_s is also estimated and in Cirrincione (2006); Lascu and Andreescu (2006); Lascu et al. (2005); Ohyama et al. (2005) which adjust the value of R_r' in proportion to the estimated R_s.

More recently, Vaclavek and Blaha (2006) developed a Lyapunov-function based flux and speed observer which can estimate R_s but not R_r', while Duran et al. (2006) performed a thermal-state estimation to compensate for the parameter and hence speed deviations due to heating.

The adaptive observer like Luenberger observer or the extended Kalman filter (Bajoi et al., 2008; Bose, 2003) gets accurate estimates under detuned operating conditions. The key issue of the adaptive observers is the computation of their gain matrix to get stability and optimum filtering when both inputs and outputs are corrupted by noise. These solutions are computationally intensive, require more memory space and are difficult to tune because the initial values of three covariance matrices have to be assumed and selected after much trial and error. So their application in low cost drives is limited.

The model reference adaptive system is also an adaptive observer technique (Maiti et al., 2008), where the same quantity is calculated by two different ways. One of them is independent of variable to be estimated while the other one is dependent on it. The two computed quantities are used to formulate the error signal. The error signal is then fed to an adaptation mechanism which in most cases is a PI controller. The output of the adaptation mechanism is the estimated quantity. One more sensorless control strategy has been suggested by Kwon and Kim (2007), where the dc link voltage is used as a control variable.

While all the speed sensorless techniques eliminate the use of mechanical speed sensor, they require the stator current and stator voltage signals as input. This requires at-least two current sensors and two voltage sensors on the stator side. Further, the output of same current sensors can be used for current regulation in the controller algorithm.

However, it is difficult to get current sensors with equal gains over the wide range of frequencies, voltages and currents used in a practical inverter. The problem is exacerbated if the motor windings are not perfectly balanced or if the current sensors have some dc offset.

Over last few years, techniques of phase current reconstruction from the dc link current have been suggested in literature which are then used for current regulation (Kim and Jahns, 2006a, b; Saritha and Janakiraman, 2007a, b; Ying and Ertugrul, 2006).

This needs only one current sensor in the dc link so that, intrinsically all the three ac line currents are measured with the same gain and no dc offset can occur. Further, the same dc current sensor can also be used to detect a shoot-through condition and subject to some restraints, a fault-to-ground.

In this paper, a new control strategy is proposed that includes the speed control, torque control and current regulation without using the mechanical speed sensor. Unlike closed loop observers, it requires less computation and is less dependent on machine parameters. Like FOC, the control is provided with variables in synchronously rotating reference frame.

However, unlike FOC, instead of having a close loop flux control, a reference value of flux is directly used to generate the d-axis component of command current. It is intentionally done to eliminate an additional PI controller and reduce the com-putational burden.

This strategy uses the dc link current and dc link voltage which are readily available for protection purposes, to implement the close-loop torque control. The stator currents and stator voltages are recon-structed from dc link quantities and the inverter switching signals. For faithful reconstruction of currents, use of adaptable gain band-pass filter is proposed in the scheme. The proposed scheme can be regarded as an improvement over the v/f control method due to the provision of torque control and current regulation.

Thus, it is suitable for low-cost, moderate performance, sensor-less IM drive applications.

The proposed drive is modeled in Matlab/Simulink software for a 2.2 kW induction motor. The simulation results are presented to verify the workability of proposed strategy.

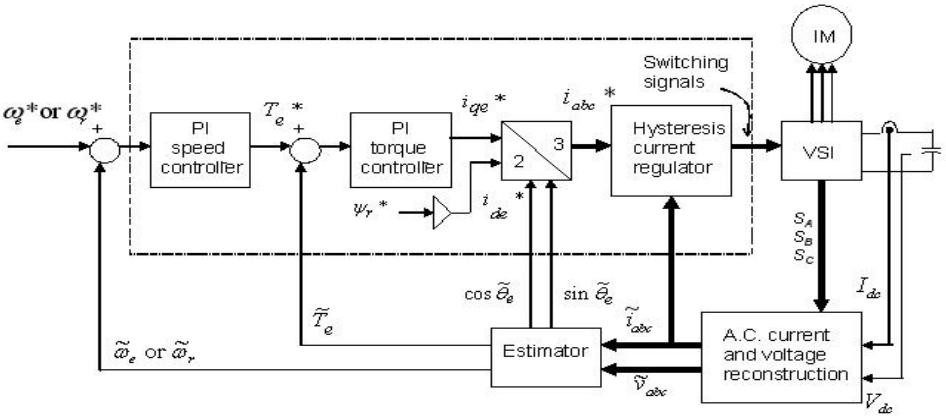

Figure 1. Block diagram of the proposed scheme.

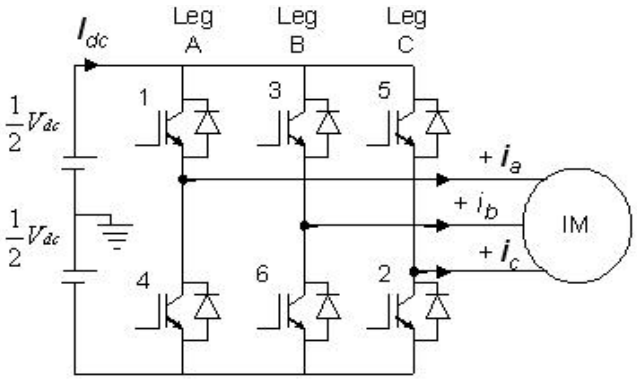

Figure 2. Voltage source inverter-induction motor drive.

PROPOSED SCHEME

Figure 1 shows the block diagram of the proposed scheme. It consists of a speed/frequency loop, a torque loop and a current regulator. The output of speed/ frequency regulator represents the torque reference for the torque loop. The torque regulator generates the q-axis current command i_{qe}* while the d-axis current command i_{de}* is directly generated from the reference rotor flux ψ_r* as given by equation (1) (Bose, 2003).

These dc commands expressed in synchronously rotating reference frame are transformed to the three phase current commands which are than compared with the actual three-phase currents (reconstructed waveforms) in a hysteresis band current regulator to generate the switching signals for the inverter. In the proposed scheme, all the feedback signals including the stator currents and stator voltages are estimated/ reconstructed from the dc link quantities.

$$i_{de}^{*} = \frac{\psi_r^{*}}{L_m} \quad (1)$$

RECONSTRUCTION OF STATOR VOLTAGES AND CURRENTS FROM DC LINK

As indicated by Boldea and Nasar (2006) and Bose voltage by inverter (2003), the stator flux, the torque and the speed can be derived from the stator voltages and currents expressed in d-q reference frame. The phase currents and voltages are related to the dc link current and switching states. A voltage source inverter-induction motor drive is shown in Figure 2 where V_{dc} is the dc link voltage, I_{dc} is the instantaneous dc link current and $i_{a,b,c}$ are the instantaneous three-phase winding currents.

Generally, IGBTs associated with snubber protection and feedback diode are used as switch in inverters. When a switch is being turned-on and the conducting diode at the same leg is being blocked off by this turn-on, because of the reverse recovery effect of diode, this leg is in fact shorted through at this moment such that a positive current spike will appear at the dc link side.

To establish the basic relationship between dc link current, winding currents and inverter switching pattern, the switches shown in Figure 2 are considered as ideal, the diode recovery effect and the snubber action are not considered either.

Space vectors

During normal state, there are eight switching states of inverter which can be expressed as space voltage vector ($S_{A,B}$ and $_C$) such as (0,0,0), (0,0,1), (0,1,0), (0,1,1), (1,0,0), (1, 0,1), (1,1,0) and (1,1,1). S_A = 1 means upper switch of leg A is on while the lower one is off, and vice versa. The same logic is applicable to S_B and $_C$ also. Amongst above eight voltage vectors, (0, 0, 0) and (1, 1, 1) are termed as zero vectors while the other six as active vectors. The switching vectors describe the inverter output voltages as shown in Figure 3.

Basic principle of phase voltage and current reconstruction: For different voltage vectors, the phase voltage that will

Table 1. DC-link current and phase voltages corresponding to active voltage vectors.

Voltage Vector ($S_{A,B,C}$)	v_a	v_b	v_c	I_{dc}
(0,0,0)	0	0	0	0
(0,0,1)	$-V_{dc}/3$	$-V_{dc}/3$	$2V_{dc}/3$	$+ i_c$
(0,1,0)	$-V_{dc}/3$	$2V_{dc}/3$	$-V_{dc}/3$	$+ i_b$
(0,1,1)	$-2V_{dc}/3$	$V_{dc}/3$	$V_{dc}/3$	$- i_a$
(1,0,0)	$2V_{dc}/3$	$-V_{dc}/3$	$-V_{dc}/3$	$+ i_a$
(1,0,1)	$V_{dc}/3$	$-2V_{dc}/3$	$V_{dc}/3$	$- i_b$
(1,1,0)	$V_{dc}/3$	$V_{dc}/3$	$-2V_{dc}/3$	$- i_c$
(1,1,1)	0	0	0	0

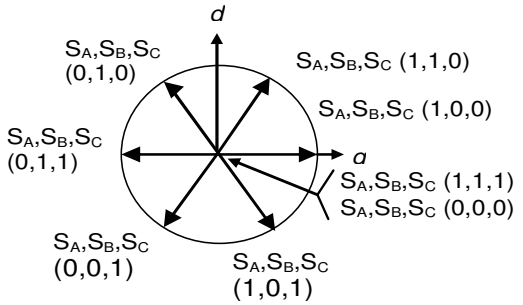

Figure 3. Voltage vectors and space sectors.

appear across stator winding can be determined by circuit observation. This is summarized in Table 1. It is assumed that the stator winding is star connected.

From above table, the expressions for the reconstruction of three phase voltages are as follows (assuming no dwelling time):

$$\tilde{v}_a = \frac{V_{dc}}{3}(2S_A - S_B - S_C) \quad (2)$$

$$\tilde{v}_b = \frac{V_{dc}}{3}(-S_A + 2S_B - S_C) \quad (3)$$

$$\tilde{v}_c = \frac{V_{dc}}{3}(-S_A - S_B + 2S_C) \quad (4)$$

These stator voltages when expressed in stationary d-q frame can be written as:

$$\tilde{v}_{qs}{}^s = \tilde{v}_a = \frac{V_{dc}}{3}(2S_A - S_B - S_C) \quad (5)$$

$$\tilde{v}_{ds}{}^s = \frac{1}{\sqrt{3}}(\tilde{v}_b - \tilde{v}_c) = \frac{V_{dc}}{\sqrt{3}}(S_B - S_C) \quad (6)$$

The relationship between the applied active vectors and the phase currents measured from the dc link sensor is also shown in Table 1. It is clear that at most, one phase current can be related to the dc link current at every instant. The reconstruction of phase currents from the dc link current can be achieved easily only if two active vectors are present for at least enough time to be sampled.

Fortunately, as indicated by Vas (1998), for most PWM strategies, two phase currents can be sampled by looking at the dc link current over every PWM period. If the PWM frequency is high enough, the phase current does not change much over one PWM period. Hence, a reconstructed current derived from the dc link current gives a reasonable approximation of the actual current. In terms of switching states and I_{dc}, the three ac line currents can be derived as follows:

$$\tilde{i}_a = I_{dc}(S_A - \frac{S_B}{2} - \frac{S_C}{2}) \quad (7)$$

$$\tilde{i}_b = I_{dc}(-\frac{S_A}{2} + S_B - \frac{S_C}{2}) \quad (8)$$

$$\tilde{i}_c = I_{dc}(-\frac{S_A}{2} - \frac{S_B}{2} + S_C) \quad (9)$$

These stator currents when expressed in stationary d-q frame can be written as:

$$\tilde{i}_{qs}{}^s = \tilde{i}_a; \quad \tilde{i}_{ds}{}^s = \frac{1}{\sqrt{3}}(2\tilde{i}_b + \tilde{i}_a) \quad (10)$$

$$\text{or } \tilde{i}_{qs}{}^s = \tilde{i}_a; \quad \tilde{i}_{ds}{}^s = \frac{-1}{\sqrt{3}}(2\tilde{i}_c + \tilde{i}_a) \quad (11)$$

$$\text{or } \tilde{i}_{qs}{}^s = -(\tilde{i}_b - \tilde{i}_c); \quad \tilde{i}_{ds}{}^s = \frac{1}{\sqrt{3}}(\tilde{i}_b + \tilde{i}_c) \quad (12)$$

There are various switching techniques (Vas, 1998) for the inverter which shall improve the performance of IM

over entire modulation range. The space vector modulation (SVM) is one of them and it has advantage of controlled switching state pattern. The current reconstruction from these switching states is feasible and can be implemented. This technique however, has some limitations and needs observer to compensate for it (Sonnaillon et al., 2006). These limitations are due to very short duration of inverter switching states; as a result, the line currents are not measurable in the dc link.

In this paper, the operation of voltage source inverter operated in current controlled mode is proposed. It is implemented by using hysteresis controller (Rashid, 2005). This makes the dc link current pulse pattern irregular but it is available for reconstruction under complete modulation range. The dc link current pulses depend on the machine parameters and the hysteresis-band (HB) in hysteresis controller. The reconstructed currents shall be affected by HB, by adjusting the HB to appropriate value; the reconstruction of line currents is possible over the entire operating speed. This is discussed ahead in detail with the help of simulation studies.

Filter

The dc link current I_{dc} consists of a train of short duration pulses and has information about the stator currents of all the three phases. By using equations 7 - 9, these pulses can be segregated into three ac line currents. Generally, an active or passive-type low-pass filter (LPF) with narrow bandwidth is used to filter out the high frequency components in the ac current waveforms thus obtained from I_{dc}.

This filter actually works as an integrator. However, a LPF causes phase lag and amplitude attenuation that vary with fundamental frequency (Zhao and Bose, 2004). In this paper, we propose the use of band-pass filter with adaptable gain to overcome this problem. The transfer function of the filter is given below:

$$y=\left[\left(\frac{sT}{1+sT}\right)\left(\frac{T}{1+sT}\right)\right]x \tag{13}$$

Where x, y and T are input, output and time constant of the band-pass filter. For $sT >> 1$; $(1+sT) \cong 1$. Therefore,

$$y = \frac{1}{s}x \tag{14}$$

ESTIMATION OF FEEDBACK SIGNALS FROM RECONSTRUCTED QUANTITIES

The feedback signals required simulating the proposed scheme, that is, flux, torque and rotor speed are estimated as follows.

Estimation of flux

The stator flux in stationary d-q frame $\psi_{ds}^{\ s}$, $\psi_{qs}^{\ s}$ and thus ψ_s can be obtained on integration of the phase voltage minus voltage drop in the stator resistance R_s (Bose, 2003):

$$\tilde{\psi}_{ds}=\int\left(\tilde{v}_{ds}^{\ s}-R_s\tilde{i}_{ds}^{\ s}\right)dt \tag{15}$$

$$\tilde{\psi}_{qs}=\int\left(\tilde{v}_{qs}^{\ s}-R_s\tilde{i}_{qs}^{\ s}\right)dt \tag{16}$$

$$|\tilde{\psi}_s| = \sqrt{\tilde{\psi}_{ds}^{\ 2}+\tilde{\psi}_{qs}^{\ 2}} \tag{17}$$

$$\cos\ \tilde{\theta}_e = \frac{\tilde{\psi}_{ds}}{|\tilde{\psi}_s|} \tag{18}$$

$$\sin\ \tilde{\theta}_e = \frac{\tilde{\psi}_{qs}}{|\tilde{\psi}_s|} \tag{19}$$

Where $\tilde{\theta}_e$ is the stator flux angle with respect to the q-axis of the stationary d-q frame.

Estimation of torque

The electromagnetic torque is expressed in terms of stator currents and flux as follows (Bose, 2003):

$$\tilde{T}_e=\frac{3P}{4}\left(\tilde{\psi}_{ds}\tilde{i}_{qs}^{\ s}-\tilde{\psi}_{qs}\tilde{i}_{ds}^{\ s}\right) \tag{20}$$

Estimation of synchronous speed and rotor speed

The synchronous speed $\tilde{\omega}_e$ can be calculated from the expression of the angle of stator flux as:

$$\tilde{\theta}_e = \tan^{-1}\frac{\tilde{\psi}_{ds}}{\tilde{\psi}_{qs}} \tag{21}$$

$$\tilde{\omega}_e = \frac{d\tilde{\theta}_e}{dt} \tag{22}$$

To obtain the rotor speed $\tilde{\omega}_r$, simple slip compensation can be derived using the steady-state torque speed curve for the machine being used:

$$\tilde{\omega}_{sl} = K_s\tilde{T}_e \tag{23}$$

Where K_s = rated slip frequency divided by rated torque and it can be derived from the name plate of the machine. Alternately, if the rotor flux ψ_r is assumed constant, the slip speed can also be calculated as:

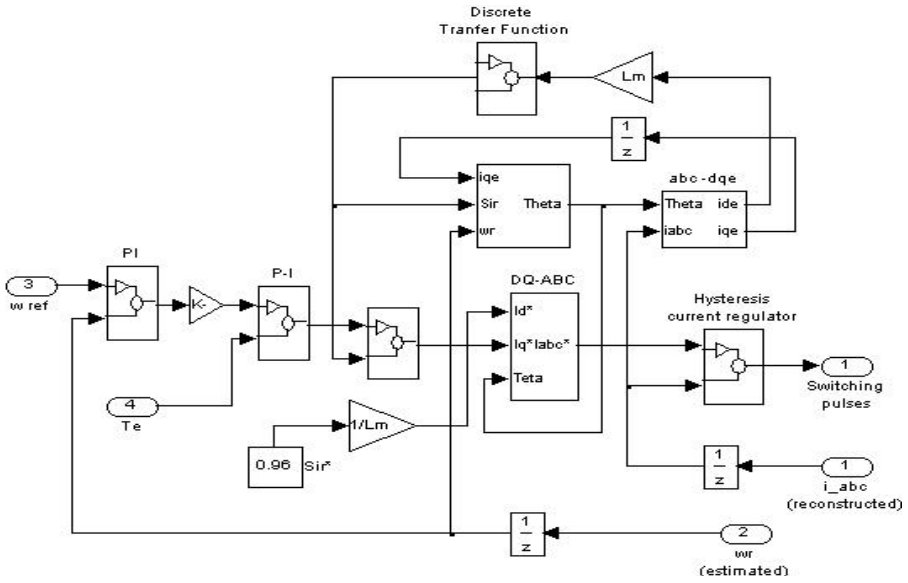

Figure 4. Simulink model of control strategy.

$$\tilde{\omega}_{sl} = \frac{R_r'}{L_r'} \frac{\tilde{i}_{qs}^{s}}{\tilde{i}_{ds}^{s}} \quad (24)$$

The rotor speed is then given by:

$$\tilde{\omega}_r = \tilde{\omega}_e - \tilde{\omega}_{sl} \quad (25)$$

PROPOSED CONTROL STRATEGY

Majority of induction motor drives are of open-loop, constant-v/f, voltage-source-inverter fed type. These drives are cost effective but they offer sluggish response. Due to high current transients during the torque changes, they are subject to undesirable trips. To avoid the unnecessary trips, the control parameters like acceleration/deceleration rate have to be adjusted (reduced) according to the load. This results in under-utilization of torque capability of the motor.

Thus, the drawback of v/f drive can be attributed to lack of torque control. This is the reason why open-loop, constant-v/f drives are mostly used in low performance fan and pump type loads (Krishnan, 2003). In this paper, we propose a modified control scheme that includes the torque control and a current regulated PWM inverter to avoid the undesirable trips due to transient currents.

As shown in Figure 1, the feedback signals, that is, torque and rotor speed are obtained from the dc link quantities. For the accuracy of these estimated quantities, the reconstructed ac line current waveforms should be correct. The accuracy of reconstructed waveforms depends upon the sampling rate (Kim and Jahns, 2006a, b; Saritha and Janakiraman, 2007b). Higher the sampling rate less is the error between the actual and reconstructed waveforms. In a hard-switching inverter, the switching frequency is limited to a typical value of a few kHz.

This limits the sampling rate of dc current and hence the update rate of torque and rotor speed using dc link quantities only. Consequently, closing the loop directly on the instantaneous value of the estimated torque now becomes difficult because estimation error during a PWM cycle could become significantly high. In fact, instantaneous error at the sampling instant could have a different polarity from the average error over one PWM cycle.

In order to use the estimated torque in a more robust manner, a control strategy should use the averaged torque instead of the instantaneous value. This leads to the control strategy depicted in Figure 1. In this system, two P-I controllers are used to regulate the average value of torque and speed respectively. The output of the P-I regulators forms the q-axis command current in a synchronously rotating reference frame.

SIMULATION STUDIES

In order to predict the behavior of the drive during steady-state and transient conditions, detailed simulation studies of the scheme shown in Figure 1 are carried out on a 3-phase, 415 V, 50 Hz and 2.2 kW induction motor by using MATLAB/SIMULINK software (Mohan, 2001). The parameters of this machine are provided in appendix.

Figure 4, shows the internal structure of the controller that consists of the speed control loop, torque control loop and the current regulation in synchronously rotating frame of reference. The switching signals for inverter are generated by comparing the command ac currents with reconstructed ac currents in a hysteresis controller. For the reconstruction of stator voltages and ac line currents, the dc link quantities are sampled with a sampling time of 2e - 6 s and then segregated into the three-phase vol-

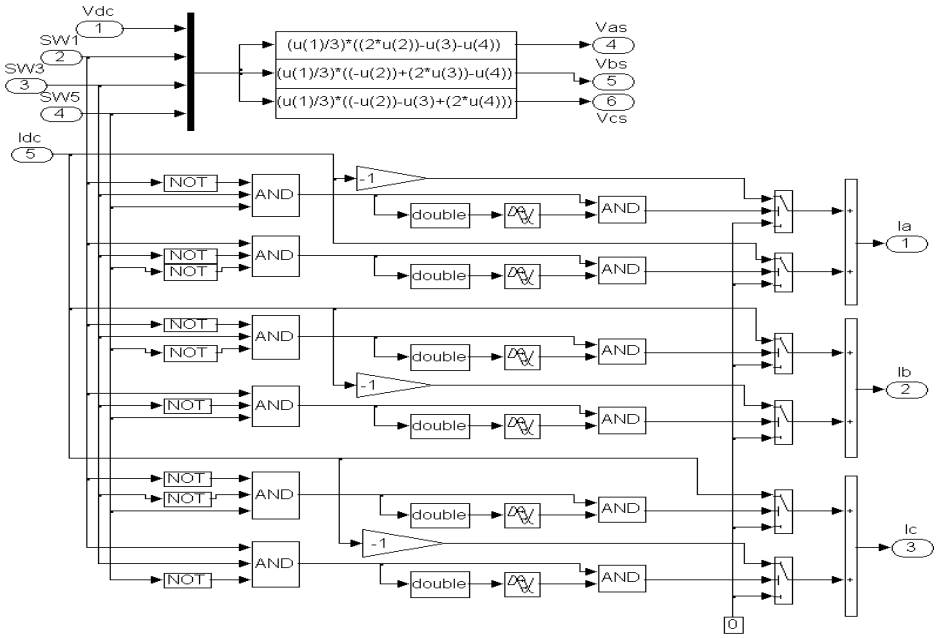

Figure 5. Simulink model for ac line currents and phase voltage reconstruction.

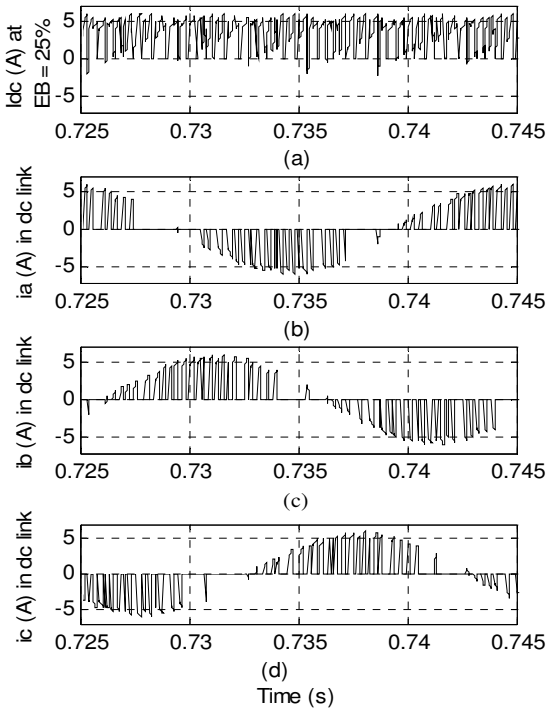

Figure 6. At rated load and HB = 25%, (a) dc link current, (b)-(d) Samples of ac line currents obtained from dc link.

tages and three ac currents as per equations 2 - 4 and 7 - 9 respectively. The simulation was carried out for five different operating conditions as is presented ahead. A variable- step ode23tb (stiff/TR-BDF2) solver was used. The model developed for this purpose is shown in Figure 5.

It is reported by Sonnaillon et al. (2006) that, in SVM, when the voltage reference is in same direction as one of the six fundamental vectors or during low modulation index or during over-modulation, the acquisition time is too short and the line currents cannot be measured from the dc link. This means that, during such durations, no samples of line currents can be obtained from the dc link and therefore their reconstruction is difficult. Practically this situation may arrive at low speeds because low-voltage reference at low speeds results in narrow pulses.

In this case, the reconstructed line currents may not be updated for a longer time because of these narrow missing pulses. In the present work, to test the feasibility of proposed scheme, such situations are simulated by selecting different values of HB. At high values of HB, the discontinuity in the switching pulses generated by hysteresis controller is more while its low values results into more number of pulses spread over the entire cycle of line currents. Selection of appropriate HB for a given application can be done by trial and error.

Figure 6 presents the waveforms of dc link current and three ac line currents as reflected in the dc link at a higher value of HB that is equal to 25% of motor rated current. The same quantities at low value of HB that is equal to 2% of motor rated current are presented in Figure 7. In both cases, the load on the shaft is assumed to be of rated value. The reconstructed phase voltages obtained as per equations 2 - 4 are shown in Figure 8. From these waveforms, it is clear that the samples of line

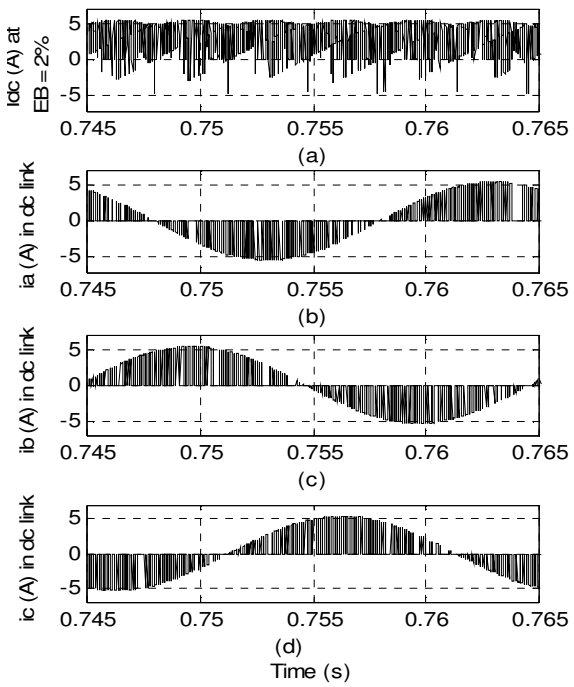

Figure 7. At rated load and HB = 2%, (a) dc link current, (b)-(d) Samples of ac line currents obtained from dc link.

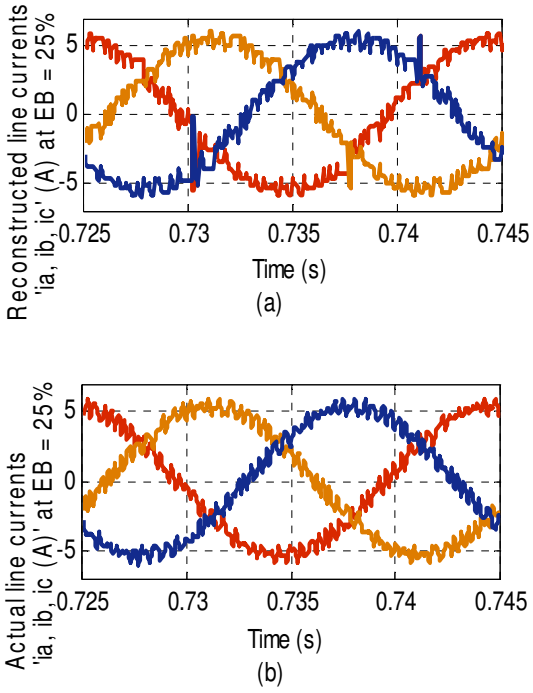

Figure 9. Line currents at rated load and HB = 25% (a) Reconstructed waveforms, (b) Actual waveforms.

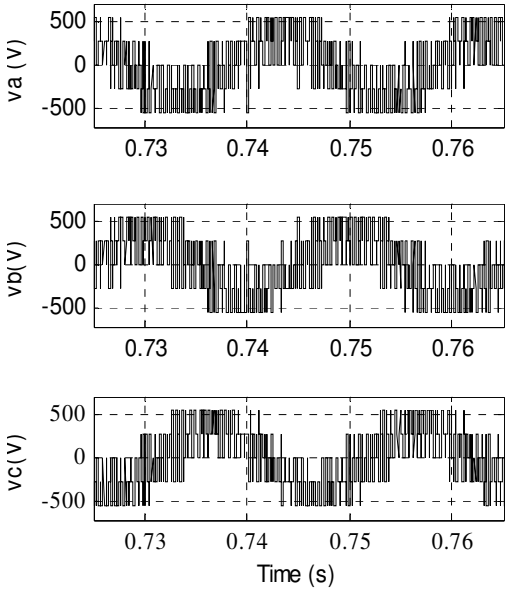

Figure 8. Reconstructed three-phase voltages at HB = 25%.

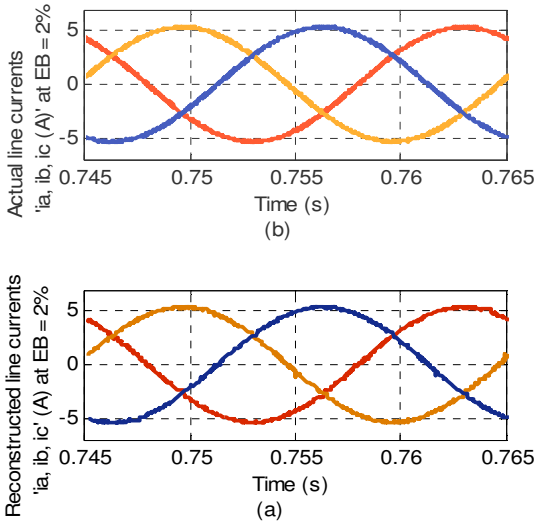

Figure 10. Line currents at rated load and HB = 2% (a) Reconstructed waveforms, (b) Actual waveforms

currents available in the dc link current are not evenly spread and being discontinuous, the set of resulting points do not constitute an acceptable reconstruction. Therefore, a zero-order hold is employed followed by a band-pass filter. The values of time constants T for the band-pass filter are selected by trial and error. The output of band-pass filter represents the reconstructed ac line currents. For above considered, values of HB (2 and 25%of motor rated current), these outputs are shown in Figures 9a and 10a respectively. For the sake of comparison, the actual ac line currents are given in Figures 9b and 10b respectively. The reconstructed and actual waveforms of line currents during 100% speed reversal at no-load are presented in Figures 11a and b. The res-

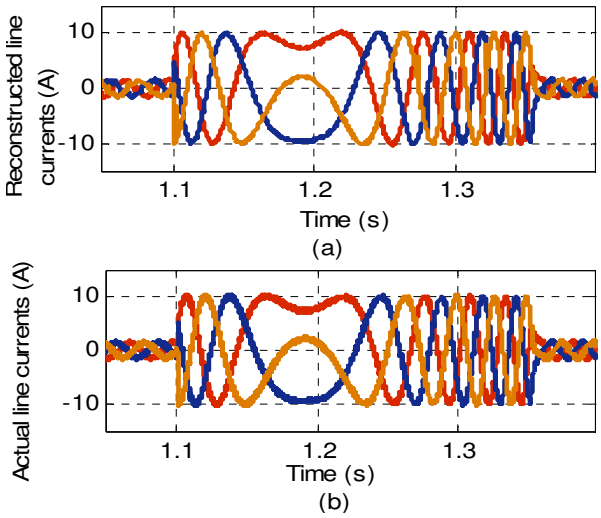

Figure 11. Line currents during 100% speed reversal at no-load condition and HB = 2% (a) Reconstructed waveforms and (b) Actual waveforms

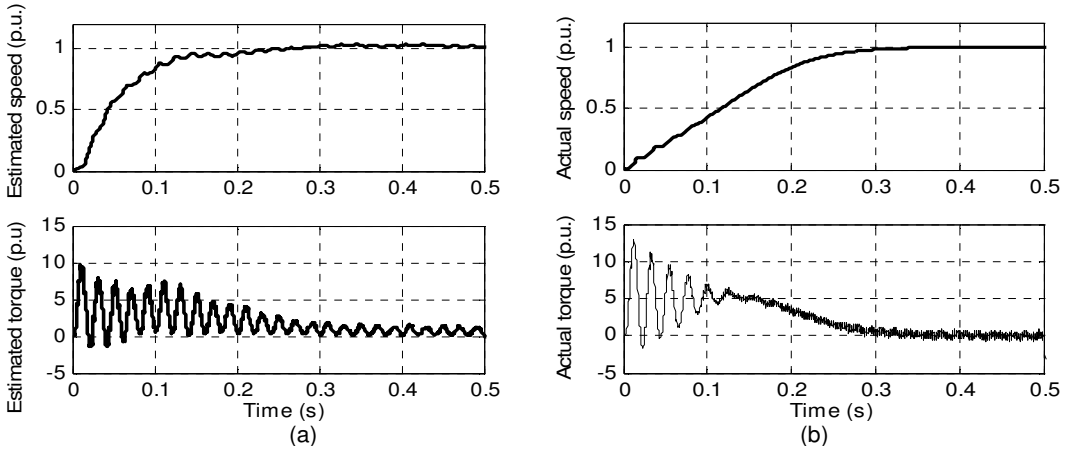

Figure 12. Free-acceleration characteristics (a) Estimated values, (b) Actual values.

ponse of speed sensorless drive during free acceleration, for step change in reference speed, step change in load, reversal of rotor speed and low speed operation is studied. To check the accuracy of estimated variables, these variables were obtained by two different ways. In the first one, the machine variables which include the flux, torque, synchronous-speed, slip-speed and rotor-speed are estimated from the dc link quantities by using equations 15 - 25 while in the second approach, these variables were calculated by using the stator currents and voltages measured directly. The simulation results of the first method were treated as estimated values while those of the latter method as actual values.

RESULTS AND DISCUSSION

Simulations, using MATLAB software package, have been carried out to verify the effectiveness of the proposed scheme. The application of proposed reconstruction technique and estimation of feedback signals is illustrated by a computer simulation as shown in the block diagram of Figure 1. The motor data used in the simulation is given in appendix. Flux reference is set to its rated value of 0.96 Wb and the dc link voltage is 600 V. Initially the speed reference is set to its rated value of 314 rad/s (treated as +100% speed reference) and it is then changed in steps to study the response as given below. The load torque is varied from zero to rated load 11.9 Nm at 0.5 s in case 4. The initial state vector is set to zero. The sampling time is set to 2e - 6. To obtain the values in per unit, the rated values were selected as base values.

Case 1: Free acceleration characteristics

The machine was allowed to accelerate from zero speed to rated speed at no-load. The steady-state was reached at 0.3 s. The waveform of estimated speed show faster response (less damped) as compared to its actual counterpart. This is shown in Figures 12a and b.

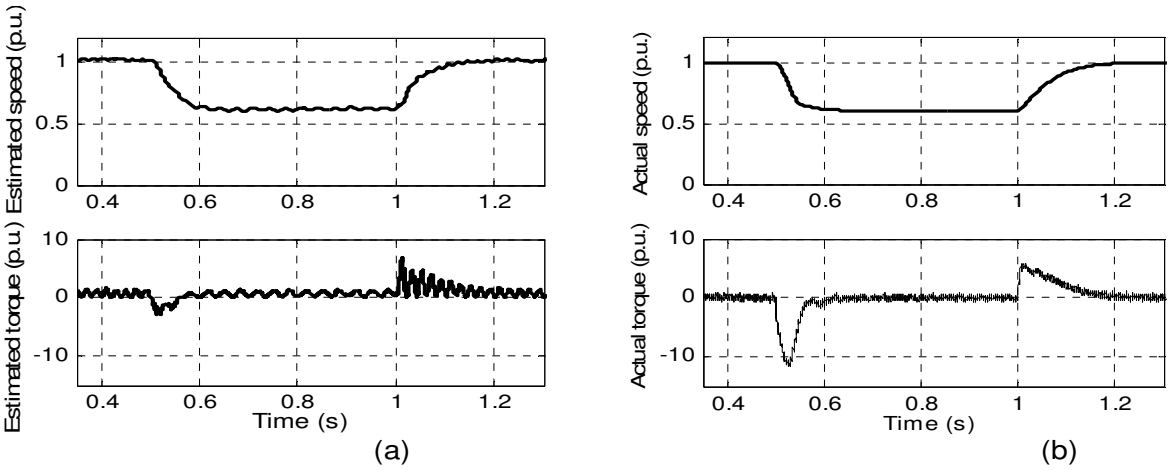

Figure 13. Variation in rotor speed and electromagnetic torque for step changes in reference speed (a) Estimated values, (b) Actual values.

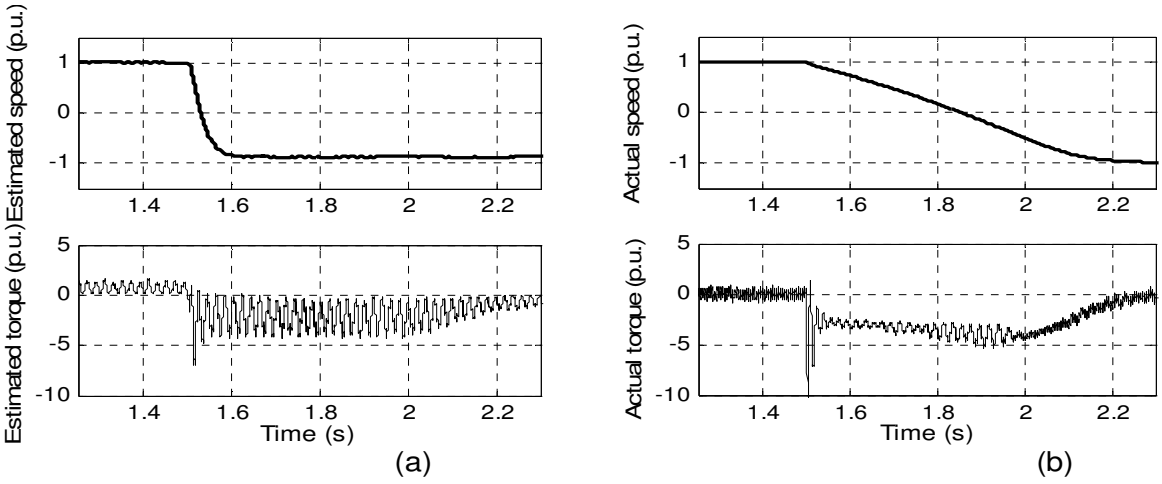

Figure 14. Variation in rotor speed and electromagnetic torque during reversal (a) Estimated values, (b) Actual values.

Case 2: Step change in speed reference

Step change in speed reference was applied two times. At 0.5 s, from +100 to +60% and vice-versa at 1 s was applied. The response is shown in Figure 13. The torque becomes negative during the first change to decelerate the motor. Upon reaching steady state, the torque becomes equal to the load torque. The response time of the drive for this step change is 100 ms. The estimated values of torque and speed vary in accordance with their corresponding actual values.

Case 3: Speed reversal

A step change in speed reference from +100 to -100% is applied at 1.5 s. This step change is equivalent to 100% speed change. The response is shown in Figure 14. The phase sequence reverses to rotate the motor in reverse direction. The drive reaches steady-state for this changes in 700 ms. This proves that the speed estimation is stable even at very low speeds.

Case 4: Step change in load

A step change in load is applied at 0.5 s. The response of the drive is shown in Figure 15. The electromagnetic torque increases to correct the speed error. Upon reaching the steady state, the torque becomes equal to the load torque. The rotor speed, after an initial droop attains back its earlier speed approximately. The motor reaches the steady state in 300 ms.

Case 5: Low speed operation

The response of the drive at 40 and 20% of rated speed is shown in Figure 16. The speed estimation is very sta-

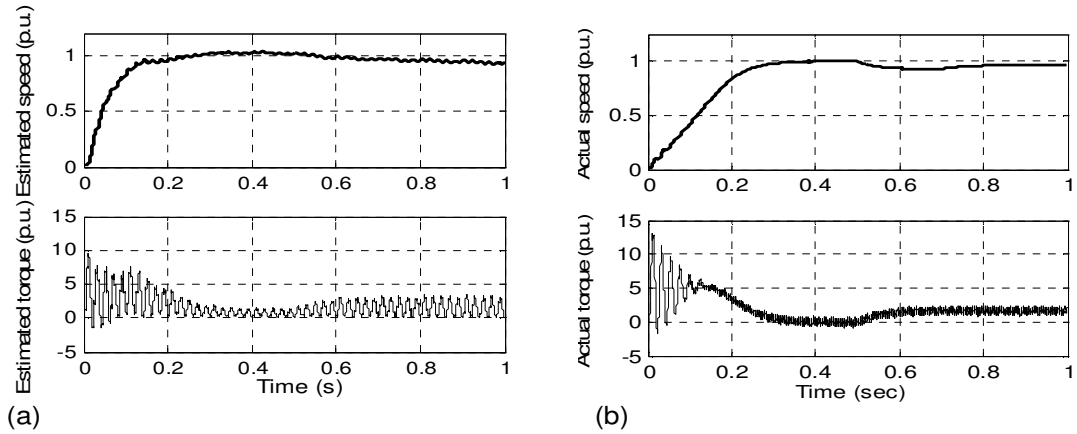

Figure 15. Variation in rotor speed and electromagnetic torque for step change in load (a) Estimated values, (b) Actual values.

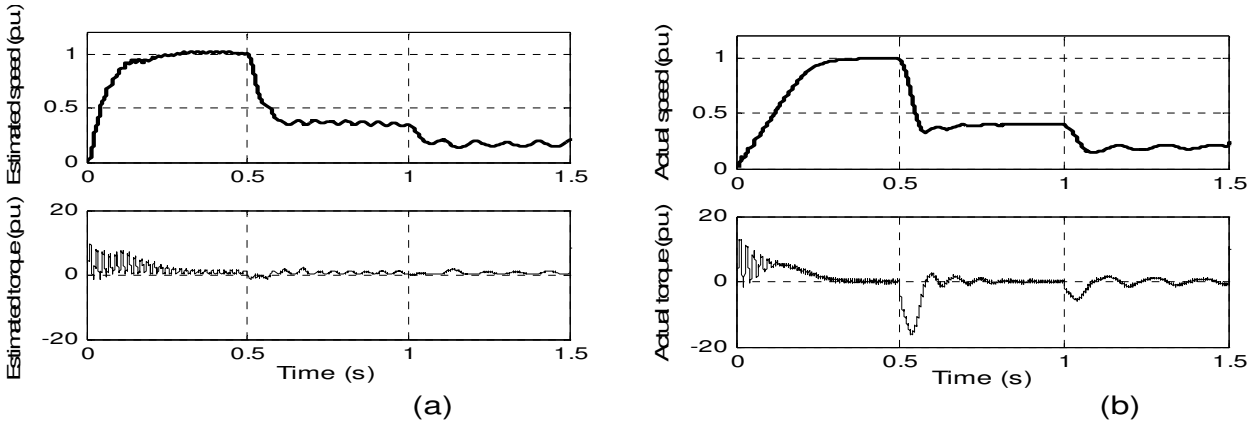

Figure 16. Variation in rotor speed and electromagnetic torque at low speeds (a) estimated values, (b) actual values.

Therefore, for fast dynamic performance, a fast update rate of estimated torque and flux is necessary. This in turn requires fast reconstruction of voltages and currents. In the present work, there is no flux-loop thus eliminating an additional PI controller and its associated computational delay. Realizing that the torque information is derived from the inverter dc link voltage and current, in a real-time system, high switching frequency shall yield high sample rate required for the estimated torque.

In the simulation study presented above, low value of HB resulted in high switching frequency of the order of 20 - 25 kHz and thus faster estimation of electromagnetic torque. The closure of current loop to control the torque results in sampling of phase current at PWM frequency. Some errors between the actual currents and the reconstructed currents may exist. In order to reduce the sensitivity to the error in reconstructed current signals, a band-pass filter is used instead of low-pass filter. This minimizes the problems of phase delay and attenuation of output signal produced by a low-pass filter.

Conclusion

In this paper, a new control strategy for induction motor drive is proposed. The drive is operated under torque control with an outer speed loop and is very similar to open-loop v/f drive in terms of power components and sensors required. Due to the inclusion of torque control loop, the drive response is fast and stable. Simulation results confirm the effectiveness of the proposed scheme.

The technique uses only dc link voltage and dc link current measurements to generate the estimates of phase voltages, line currents, flux, torque and rotor speed. If the dc link voltage is assumed as constant, only one current sensor in the dc link is sufficient to give the estimates of all required feedback variables.

Moreover, the same current sensor that is already available in the dc link of an open-loop v/f drive for protection purpose can be used. Thus, the open-loop control strategy in an existing v/f drive can be replaced by the

proposed close-loop control strategy without requiring any additional power components or the physical sensors. The proposed strategy appears to be a good compromise between the high-cost, high-performance field-oriented drives and the low-cost, low-performance v/f drives.

Practical implementation of the proposed scheme on a 16 bits floating point arithmetic Texas Instrument TMS320C31 processor are the subject of future follow-up research work.

APPENDIX

Motor data

Rated voltage = 415V (L-L)
Rated current = 4.8A
R_s = 11.1
L_m = 0.71469
$L_{s=}$ 0.7329
L'_r = 0.7329
R'_r = 2.2605
P = 4

REFERENCES

Bojoi R, Guglielmi P, Pellegrino G (2008). Sensorless direct field-oriented control of three-phase induction motor drives for low-cost applications, IEEE Trans. Ind. Appl. 44(2): 475-481.

Boldea I, Nasar SA (2006). Electric Drives, Taylor & Francis, New York.

Bose BK (2003). Power Electronics and Motor Drives, Pearson Education, Inc, Delhi, India. pp. 333 - 404.

Boussak M, Jarray K (2006). A high-performance sensorless indirect stator flux orientation control of induction motor drive, IEEE Trans. Ind. Electron 53(1): 41-49.

Cirrincione M, Pucci M, Cirrincione G, Capalino GA (2006). An adaptive speed observer based on a new total least- squares neuron for induction machine drives. IEEE Trans. Ind. Appl. 42(1): 89-104.

Comanescu M, Xu L (2006). An improved flux observer based on PLL frequency estimator for sensorless vector control of induction motors, IEEE Trans. Ind. Electron 53(1): 50-56.

Derdiyok A (2005). Speed-sensorless control of induction motor using a continuous control approach of sliding-mode and flux observer. IEEE Trans. Ind. Electron 52(4): 1170-1176.

Duran MJ, Duran JL, Perez F, Fernandez J (2006). Induction-motor sensorless vector control with on-line parameter estimation and over-current protection, IEEE Trans. Indian Electron 53(1): 154-161.

Guidi G, Umida H (2000). A novel stator resistance estimation method for speed-sensorless induction motor drives, IEEE Trans. Ind. Appl. 36(6): 1619 - 1627.

Harnefors L, Jansson M, Ottersten R, Pietilainen K (2003). Unified sensorless vector control of synchronous and induction motors, IEEE Trans. Ind. Electron. 50(1): 153-160. In: PMAC motors, Proc. of IPEMC 2006, International Power Electronics and Motion Control Conf.1: 1-5, Shangai, China.

Kim Hongrae, Jahns Thomas M (2006a). Phase current reconstruction for AC motor drives using a DC link single current sensor and measurement voltage vectors, IEEE Trans. Power Electron 21(5): 1539-1546.

Kim Hongrae, Jahns Thomas M (2006b). Current control for AC motor drives using a single dc-link current sensor and measurement voltage vectors, IEEE Trans. Ind. Appl. 42(6): 1539 - 1546.

Krishnan R (2003). Electric Motor Drives-Modeling, Analysis and control, Pearson Education, Inc., Delhi, India. pp. 128 - 215.

Kwon Young Ahn, Kim Sang Kyoon (2007). A high-performance strategy for sensorless induction motor drive using variable link voltage, IEEE Trans. Power Electron 22(1): 329-332.

Lascu C, Andreescu GD (2006) Sliding-mode observer and improved observer with DC-offset compensation for flux estimation in sensorless- controlled induction motors, IEEE Trans. Ind. Electron. 53(3): 785-794.

Lascu C, Boldea I, Blaabjerg F (2004). Direct torque control of sensorless induction motor drives: A sliding mode approach, IEEE Trans. Ind. Appl. 40(2): 582-590.

Lascu C, Boldea I, Blaabjerg F (2005). Very-low-speed variable-structure control of sensorless induction machine drives without signal injection, IEEE Trans. Ind. Appl. 41(2): 591-598.

Maiti S, Chakraborty C, Hori Y, Ta Minh. C (2008). Model reference adaptive controller-based rotor resistance and speed estimation techniques for vector controlled induction motor drive utilizing reactive power, IEEE. Trans. Ind. Electron 55(2): 594-601.

Messaoudi M, Sbita L, Abdelkrim MN (2007). A robust nonlinear observer for states and parameters estimation and on-line adaptation of rotor time-constant in sensorless induction motor drives, Intl. J. Phys. Sci. 2(8): 217-225.

Mohan M (2001). Simulation of sensorless vector control of induction motor using MATLAB/SIMULINK, Matlab India Millennium Conference. pp. 78-84.

Nagata K, Okuyama T, Nemoto H, Katayama T (2008). A simple robust voltage control of high power sensorless induction motor drives with high start torque demand, IEEE Trans. Ind. Appl. 44(2): 604-611.

Ohyama K, Asher GM, Sumner M (2005). Comparative analysis of experimental performance and stability of sensorless induction motor drives, IEEE Trans. Ind. Electron. 53(1): 178-186.

Rashid M (2005). Power Electronics- Circuits, Devices and Applications, Prentice-Hall of India Pvt. Ltd., New Delhi, India. pp.264-265.

Rodic M, Jezernik K (2002). Speed-sensorless sliding-mode torque control of induction motor, IEEE Trans. Ind. Electron. 49(1): 87-95.

Saritha B, Janakiraman PA (2007a). An observer for three-phase current estimation using non-uniform current samples, IEEE Trans. Power Electron 22(2): 686-692.

Saritha B, Janakiraman PA (2007b). Sinusoidal three-phase current reconstruction and control using a dc-link current sensor and a curve-fitting observer, IEEE Trans. Ind. Electron 54(5): 2657-2662.

Sonnaillon MO, Bisheimer G, Angelo De, Solsona J, Garcia GO (2006). Mechanical-sensorless induction motor drive based only on DC-link measurements, IEE Proc. Electr. Appl. 153(6): 815-822.

Tzou YY, Hsu HJ (1997). FPGA realization of space-vector PWM control IC for three-phase PWM inverters, IEEE Trans. Power Electron 12(6): 953-963.

Vaclavek P, Blaha P (2006). Lyapunov-function-based flux and speed observer for AC induction motor sensorless control and parameter estimation, IEEE Trans. Ind. Electron. 53(1): 138-145.

Vas P (1998). Sensorless Vector and Direct Torque Control, Oxford Science, Oxford, U.K Pp. 123-184.

Ying L, Ertugrul N (2006). An observer-based three-phase current reconstruction using DC link measurement In: PMAC motors, Proc. of IPEMC 2006, International Power Electronics and Motion Control Conf. Shangai, China. 1: 1-5.

Zhao J, Bose BK (2004) Neural-network-based waveform processing and delay-less filtering in power electronics and AC drives, IEEE Trans. Ind. Electron. 51(5): 981-991.